Effect of hydrogen on Ni/Ti multilayer neutron monochromator performance

Hyunsu Ju and Brent J. Heuser[a)]
Department of Nuclear, Plasma, and Radiological Engineering, University of Illinois, Urbana, Illinois 61801

(Received 3 November 2006; accepted 3 January 2007; published online 15 February 2007)

Ni/Ti multilayers with and without hydrogen added to the Ti layers have been prepared by dc-magnetron sputtering to investigate the effect of hydrogen on neutron monochromator performance. The addition of hydrogen further reduces the negative scattering length density of Ti, thereby increasing the contrast with the Ni. Increases in the first order peak reflectivity by factors of 2–3 have been observed in neutron reflectivity measurements. The improved performance is attributed to a larger neutron scattering length density contrast and to a sharpening of the interfaces. © *2007 American Institute of Physics*. [DOI: 10.1063/1.2437691]

Nonpolarizing neutron optical devices, such as monochromators and supermirrors, typically employ Ni and Ti when fabricated with thin-film architecture,[1–5] although alternative systems are possible.[6,7] The ability of a multilayer optical device to deliver on-sample intensity is related to the scattering length density (SLD) contrast between the alternating layers of the deposition and to the sharpness of the interfaces.[8] Recent efforts to improve interfacial sharpness of Ni/Ti multilayers using interdiffusion barriers such as Cr (Ref. 9) and C (Refs. 4 and 10) have been effective to a limited degree. Past efforts to improve the layer contrast by the addition of H to Ti in the Ni/Ti multilayer system[3] yielded inconclusive results, as discussed below. Here we present a systematic study of the effect of H addition on Ni/Ti multilayer performance.

Two series of Ni/Ti multilayers, with and without H, have been prepared by dc-magnetron sputtering at room temperature without active cooling on (100) Si substrates (native oxide present) with a deposition rate of 1 Å/s under 3 mTorr total gas pressure at a flow rate of ~60 SCCM (SCCM denotes cubic centimeter per minute at STP) using an AJA 2000 cosputtering system. The number of bilayers (BL) was varied from 2 to 40 BL. All depositions started with Ti and ended with Ni, resulting in good adhesion, lower postdeposition oxidation rates. The presence of Ni, with effectively zero H solubility, prevented H loss in air or under vacuum. Pure Ar gas was used to deposit the without-H series, while a 90%–10% mixture of Ar–H gas during Ti deposition only was used for the with-H series. X-ray diffraction analysis (not shown) confirmed the presence of the TiH_2 hydride phase when H_2 gas was present during deposition. All samples were rotated during fabrication to improve uniformity. A liquid nitrogen coolant coil surrounding the target-substrate region was used to getter oxygen. The typical thickness of each layer was 40 Å (80 Å bilayer thickness or multilayer period), although variations from sample to sample existed. The 80 Å period corresponds to a wave vector transfer of $Q=0.08$ Å^{-1} [$Q=(4\pi/\lambda)\sin\theta$, where λ is the wavelength and θ is the angle between the incident beam and the sample surface] for the first order diffraction peak. The neutron reflectivity response of the samples was measured in air at ambient temperature with the POSY 2 reflectometer at the Intense Pulsed Neutron Source at Argonne National Laboratory.[11] This instrument records intensity on a one-dimensional position sensitive detector as a function of neutron time of flight with the sample at a fixed angle. Generally, three different fixed sample angles, offset by approximately 0.5°, were needed to acquire a complete reflectivity response from the critical edge plateau (total external reflection) to just beyond the first order diffraction peak. The measured reflectivity (R) was placed on an absolute scale by setting the critical edge plateau to $R=1$. The interfacial sharpness was investigated with Auger electron spectroscopy (AES) using a Physical Electronics PHI 660 scanning Auger microprobe.

The specular neutron reflectivity response from the 4, 10, and 20 BL samples with and without H is shown in Fig. 1. Slight variations in the first order peak Q value from sample to sample are evident, as is the systematic narrowing of the diffraction peak with BL number. Also notice a systematic increase in the critical edge location (maximum Q value for total external reflection) as the BL number increases, an effect due to the presence of greater amounts of Ni. Approximately 3000 Å of Ni is necessary to saturate the reflected neutron intensity at the bulk Ni critical edge ($Q=0.022$ Å^{-1}). We therefore do not expect total external reflection out to this value for our samples (~800 Å of Ni is present for the 20 BL sample, for example).

The data fits shown in Fig. 1 were obtained using the REFLPAK software suite[12] and yielded values for the neutron SLD (product of the atomic number density and the neutron bound atom coherent scattering length) for the Ni and Ti layers, the average multilayer period, and the interfacial roughness. In principle, the SLD of the Ti layers determined from these fits could serve as an independent measurement of the H concentration if the lattice expansion of the host is taken into account.[13] However, fits to specular reflectivity data are not unique, a fact that is especially true for multilayer systems where each layer and interface contribute to the overall response. In the present case, it was found that families of fits with approximately equal root-mean-squared summation values could be obtained from different SLD-interfacial roughness combinations for each sample. The best fits within these families were consistent with the theoretical SLD values of bulk Ni (9.41×10^{-6} Å^{-2}), bulk Ti (-1.95×10^{-6} Å^{-2}), and bulk TiH_2 (-5.14×10^{-6} Å^{-2}) for the

a)Electronic mail: bheuser@uiuc.edu

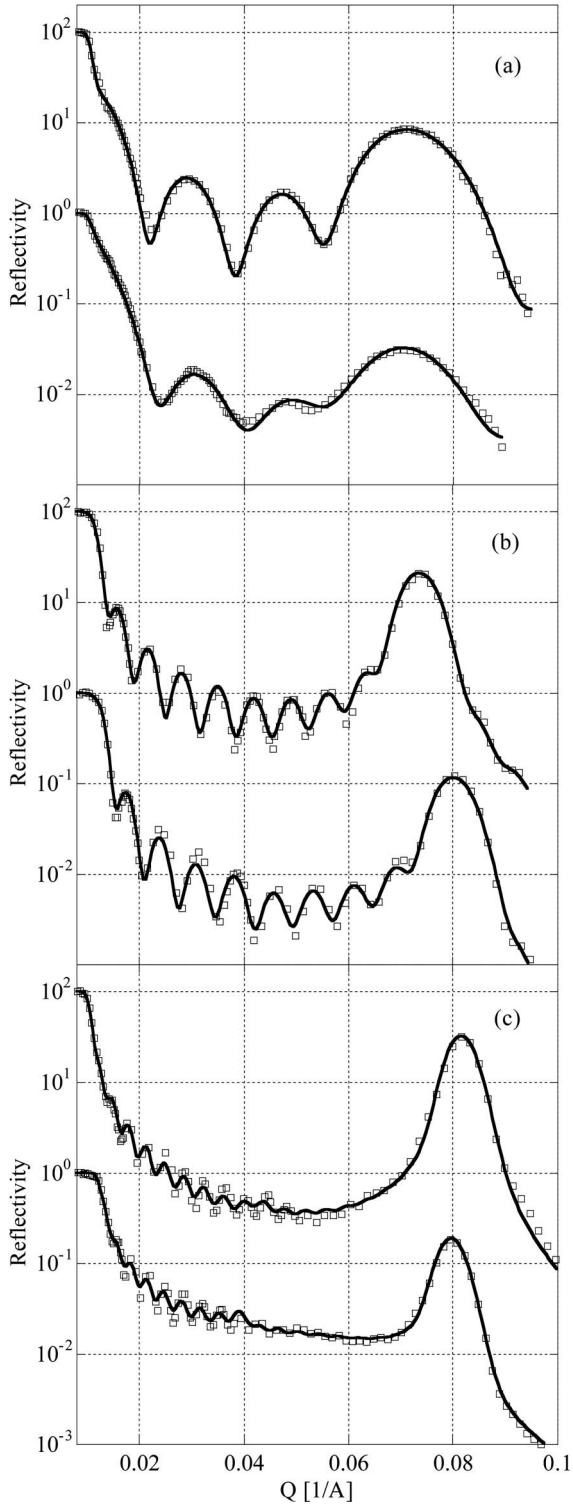

FIG. 1. Neutron reflectivity vs Q for (a) 4 BL samples, (b) 10 BL samples, and (c) 20 BL samples. The with- and without-H samples are shown as labeled. The with-H measurements have been shifted upward by 100X for clarity. The solid lines are best fits based on the solution of the one-dimensional Schrödinger equation.

with-H samples, and had interfacial half widths of order of 5–10 Å.

The absolute first order peak reflectivity (R_{max}), peak centroid (Q_{max}), and peak standard deviation (ΔQ_{max}) determined by a Gaussian fit to the measured diffraction peak are listed in Table I. The theoretical peak reflectivity from the dynamical theory result of Sears[8] for perfectly sharp interfaces is given by

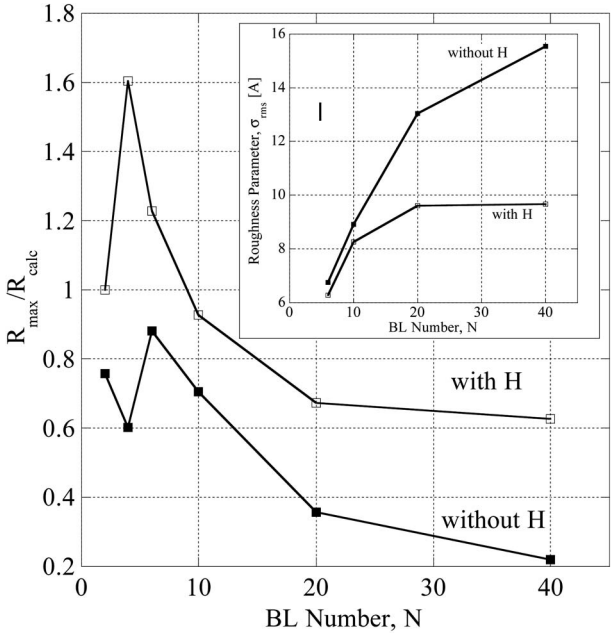

FIG. 2. Normalized first order peak neutron reflectivity vs bilayer number for the with- (open boxes) and without-H (solid boxes) samples. The measurements are normalized to the calculated Ni/Ti reflectivity to account for variation in the multilayer period. The errors associated with the normalized reflectivity values are smaller than the plotting symbols. The inset shows the Debye-Waller rms-roughness parameter for each measured peak reflectivity. A typical error bar associated with the rms-roughness calculation is shown.

$$R_{calc} = \tanh^2(2Nd^2\Delta\rho/\pi), \tag{1}$$

where N is the number of bilayers, $\Delta\rho$ is the SLD contrast between Ni and Ti, and the multilayer period is given by $d = 2\pi/Q_{max}$. The theoretical peak reflectivity, assuming bulk theoretical SLD values for Ni and Ti (not the theoretical TiH_2 value for the with-H samples), is listed in Table I. The strong dependence of the peak reflectivity on the multilayer period dictates normalization of the measured peak reflectivity by the theoretical value. This normalization is shown in the last column of Table I.

The normalized reflectivity values for both sample sets are plotted in Fig. 2. The presence of hydrogen results in a significant increase in peak reflectivity for all BL numbers. We attribute the systematic reduction in peak reflectivity with BL number for both sample sets to an increase in inter-

TABLE I. Comparison of the measured and calculated first order peak reflectivities.

Sample	R_{max}	Q_{max} (1/Å)	d (Å)	ΔQ_{max} (1/Å)	R_{calc}	R_{max}/R_{calc}
2 BL Ni/TiH_2	0.016	0.0674	93.2	0.013	0.016	1.0
4 BL Ni/TiH_2	0.077	0.0713	88.1	0.0071	0.048	1.60
6 BL Ni/TiH_2	0.081	0.0808	77.8	0.0055	0.066	1.23
10 BL Ni/TiH_2	0.215	0.0737	85.3	0.0034	0.232	0.93
20 BL Ni/TiH_2	0.323	0.0818	76.8	0.0028	0.480	0.67
40 BL Ni/TiH_2	0.587	0.0746	84.2	0.0019	0.936	0.63
2 BL Ni/Ti	0.011	0.0688	91.3	0.014	0.014	0.76
4 BL Ni/Ti	0.031	0.0703	89.4	0.0083	0.052	0.60
6 BL Ni/Ti	0.063	0.0790	79.5	0.0049	0.072	0.88
10 BL Ni/Ti	0.122	0.0803	78.3	0.0035	0.173	0.71
20 BL Ni/Ti	0.182	0.0798	78.7	0.0028	0.510	0.36
40 BL Ni/Ti	0.197	0.0798	78.7	0.0029	0.895	0.22

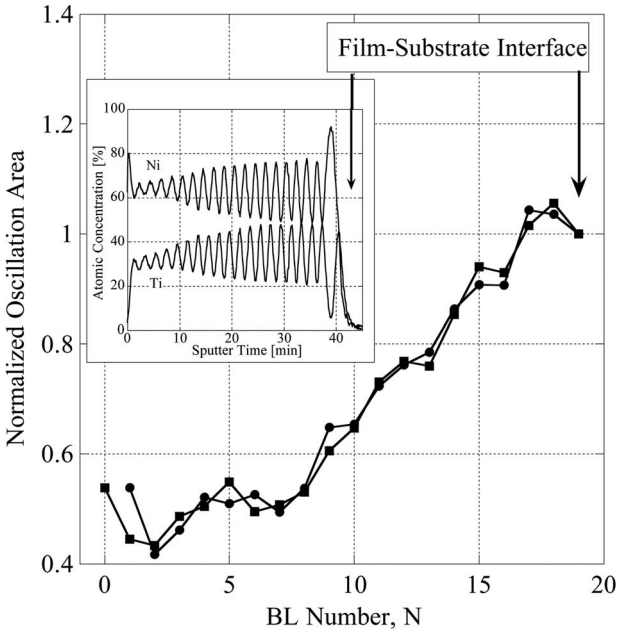

FIG. 3. Normalized AES oscillation area for Ni (solid boxes) and Ti (solid circles) vs bilayer number for the with-H 20 BL Ni/Ti sample. The inset shows Ni and Ti AES atomic concentration profiles vs sputter time.

facial roughness or blurriness beyond $N \sim 6$. The effect of the interfacial roughness on peak reflectivity can be modeled with a Debye-Waller formalism,[14]

$$R_{\max} = R_{\text{calc}} \exp(-\sigma_{\text{rms}}^2 Q_{\max}^2), \tag{2}$$

where σ_{rms} is the interfacial roughness parameter. The Debye-Waller correction can be applied to each absolute peak reflectivity measurement ($R_{\max}$) to determine the characteristic roughness for that sample. The application of this correction requires a calculated reflectivity value to determine σ_{rms}; this calculation must take into account the presence of hydrogen in the with-H samples to accurately model the effect of interfacial roughness. The H concentration in all the with-H samples was measured using a calibrated temperature programed desorption analysis apparatus. These concentrations, which were consistent with a TiH_2 stoichiometry, were then used to calculate the theoretical peak reflectivity for the with-H samples. The resulting roughness parameter values are plotted in the inset of Fig. 2. This analysis demonstrates that the interfacial roughness, as modeled with Eq. (2), increases with the BL number and that the presence of H significantly reduces the interfacial roughness for large BL numbers.

The sharpness of the interfaces was investigated with AES. Generally, AES is not an optimum probe of buried interfaces because of an ion beam mixing effect that propagates during sputtering. However, the mixing effect can be minimized by reducing the energy and angle of incidence of the sputter ion beam. The normalized area under each Ni and Ti atomic concentration oscillation in the AES profile (Fig. 3, inset) of the with-H 20 BL Ni/Ti sample is shown in Fig. 3. Similar analysis was used by Tadayyon *et al.* to study interdiffusion in Ni/Ti multilayers during annealing.[15] The normalized area increases as the film-substrate interface is reached, indicating a better interfacial sharpness. This result is therefore consistent with a better interfacial sharpness at low BL number as well.

The results of Maaza *et al.*[3] are relevant to our work. These authors measured the neutron reflectivity response from a single with-H 10 BL Ni/Ti multilayer sample. They found that annealing increased the peak reflectivity, an effect attributed to the partial redistribution of hydrogen from the Ni layers to the Ti layers. Unfortunately, these authors did not measure a without-H sample and their conclusions regarding the effectiveness of H are based solely on model fitting, a procedure that resulted in unsatisfactory agreement (in our opinion) with the data. In addition, some reflectivity data sets do not appear to be properly normalized to $R=1$ on the critical edge plateau, placing the absolute measured peak reflectivity values in doubt. We therefore consider the work of Maaza *et al.* to be inconclusive with regard to the effectiveness of H on multilayer performance.

In summary, the presence of H in the Ti layers increases the first order peak reflectivity by factors of 2–3 (after normalization) compared to the without-H case. The systematic reduction in the normalized peak reflectivity with BL number is attributed to a loss of interfacial sharpness as the number of bilayers increases. Both the AES and Debye-Waller analyses are consistent with a degradation of interfacial sharpness as the BL number increases. The Debye-Waller analysis also indicates that the presence of H results in sharper interfaces.

This work was supported by the U.S. Department of Energy Innovations in Nuclear Education and Infrastructure (INIE) Program under Contract No. PU-2406-UI-4423. This research is based upon the work supported by the U.S. Department of Energy, Division of Materials Sciences under Award No. DEFG02-91ER45439, through the Frederick Seitz Materials Research Laboratory at the University of Illinois at Urbana-Champaign. This work also benefited by the use of the IPNS funded by the U.S. Department of Energy, Basic Energy Sciences under Contract No. W-31-109-ENG-38 to the University of Chicago. The assistance of R. Goyette (ORNL) and S. Park (KBSI) is gratefully acknowledged. Finally, the authors are very grateful to N. Finnegan (UIUC) for performing the AES measurements.

[1] A. M. Saxena, J. Appl. Crystallogr. **19**, 123 (1986).
[2] T. Akiyoshi, T. Ebisawa, T. Kawai, F. Yoshida, M. Ono, S. Tasaki, S. Mitani, T. Kobayashi, and S. Okamoto, J. Nucl. Sci. Technol. **29**, 939 (1992).
[3] M. Maaza, Z. Jiang, F. Samuel, B. Farnoux, and B. Vidal, J. Appl. Crystallogr. **25**, 789 (1992).
[4] M. Hino, H. Sunohara, Y. Yoshimura, R. Maruyama, S. Tasaki, H. Yoshino, and Y. Kawabata, Nucl. Instrum. Methods Phys. Res. A **529**, 54 (2004).
[5] J. Padiyath, J. Stahn, and M. Horisberger, Appl. Phys. Lett. **89**, 113123 (2006).
[6] A. M. Saxena and B. P. Schoenborn, Acta Crystallogr., Sect. A: Cryst. Phys., Diffr., Theor. Gen. Crystallogr. **A33**, 805 (1977).
[7] A. E. Munter, B. J. Heuser, and K. M. Skulina, Physica B **221**, 500 (1996).
[8] V. F. Sears, Acta Crystallogr., Sect. A: Found. Crystallogr. **A39**, 601 (1983).
[9] M. Ay, C. Schanzer, M. Wolff, and J. Stahn, Nucl. Instrum. Methods Phys. Res. A **562**, 389 (2006).
[10] H. Takenaka, H. Ito, K. Nagai, Y. Muramatsu, E. Gullikson, and R. C. C. Perera, Nucl. Instrum. Methods Phys. Res. A **467–468**, 341 (2001).
[11] A. Karim, B. H. Arendt, R. Goyette, Y. Y. Huang, R. Kleb, and G. P. Felcher, Physica B **173**, 17 (1991).
[12] P. A. Kienzle, K. V. O'Donovan, J. F. Ankner, N. F. Berk, and C. F. Majkrzak, http://www.ncnr.nist.gov/reflpak.
[13] A. E. Munter and B. J. Heuser, Phys. Rev. B **58**, 678 (1998).
[14] B. E. Warren, *X-Ray Diffraction* (Dover, New York, 1990), p. 35.
[15] S. M. Tadayyon, O. Yoshinari, and K. Tanaka, Jpn. J. Appl. Phys., Part 1 **31**, 2226 (1992).